Oxidation and Corrosion Mechanism of Steel Alloys and Inconel 600 Alloy in Liquid–Lead-Bismuth Eutectic

Ahmed Moosa*

Received on:21/10/2007
Accepted on:5/6/2008

Abstract

The alloys used in this study were two types pf stainless steels (304SS and 316 SS) , low alloy steel (Type T_{22}-ASTM) and Inconel 600 alloy `(nickel-base superalloy). The oxidation mechanism were studied for three steel alloys and for inconel 600 in liquid Pb-Bi eutectic (LBE) in the temperature range 450- 550 ^{o}C using stagnant test . A model based on the experiments of Cr oxidation at high temperature with scale vaporization was applied to the present oxidation process by replacing the vaporization rate with the mass-transfer-corrosion rate. The results indicate that all steel alloys showed an oxidation/corrosion behavior. The oxidation kinetics is parabolic and the corrosion kinetics is linear. The parabolic oxidation rate constant are of the following order $(Kp)_{304SS}$ $(Kp)_{316SS} > (Kp)_{low\ alloy\ steel}$.
The scale-removal-rate constants *Kr* by mass transfer corrosion are of the following order $(Kr)_{inconel} > (Kr)_{316SS} > (Kr)_{304SS}$. The weight loss increases with increasing Ni content in the steel alloys.

Keywords: Oxidation, Corrosion, Liquid Metals

الخلاصة

استخدم في هذا البحث الفولاذ الغير قابل للصدا نوع 316 و304 وكذلك الفولاذ الواطي السبائكي وسبيكة الانكونيل 600 . تم دراسة الية التاكسد للسبائك في منصهر الرصاص-البزموث الايوتكتيكي في درجة حرارة 450-550 م° .تم استخدام موديل يعتمد على اكسدة الكروم في درجات حرارة عالية مع استبدال الية تبخر الكروم بالية انتقال المادة بالية التاكل .
اظهرت النتائج ان جميع السبائك الفولاذية في هذا البحث تتعرض الى تاكل /تاكسد . تشير نتائج الدراسة الحالية إلى أن السلوك الكيناتيكي العام للتأكسد للسبائك الفولاذية يتبعً قانون القطع المكافئ (Parabolic Law) . و كانت قيم ثابت معدل التأكسد (k_P) كما يلي $(Kp)_{304SS} > (Kp)_{316SS} > (Kp)_{low\ alloy\ steel}$;
ان معدل التاكل الخطي للسبائك (Kr) فهو
$(Kr)_{inconel} > (Kr)_{316SS} > (Kr)_{304SS}$
ان الفقدان في الوزن يزداد بزيادة تركيز النيكل في السبائك الفولاذية.

Introduction

Advanced nuclear reactors require the structural materials to be in contact with the molten metals/lead bismuth eutectic at 400^{0}C and at higher temperatures. One of the primary concerns in using the molten lead-bismuth eutectic (LBE) as the coolant is the degradation of structural materials in contact with LBE. Several coolant have been proposed such as, sodium and lead-bismuth alloy. Major disadvantages of the sodium coolant are treatment of chemically active sodium and the positive void reactivity. Here, molten Pb-Bi eutectic (LBE - Bi-56.1 wt.% and balance Pb, melting point 125º C) is used as a coolant [1].

The new generation of nuclear reactors must be economically competitive, inherently safe, and able to minimize waste. Among the various reactor concepts being considered, one is the lead-cooled (Pb) or lead-alloy-cooled fast reactor. Lead alloy coolants offer a number of attractive properties: chemical inertness with air and water (unlike sodium), low vapor pressure over the relevant temperature range, high boiling point (in contrast to sodium), high atomic number, and favorable neutronics in high scattering and small absorption microscopic cross sections. [2,3].

One of the key issues for the development of lead– bismuth (Pb–Bi) cooled Fast Breeder Reactors (FBRs) is the compatibility of core and structural materials with Pb– Bi flow at high temperature. The main form of corrosion is the mass transfer of cladding and structural materials along a thermal gradient, *via* dissolution in the hot regions and precipitation in the cold regions [4].

Glasbrenner et al. [5] conducted many experiments in a liquid lead pumped loop at 400°C and 550°C to examine the corrosion behavior of ferritic and austenitic steels. During exposure to liquid lead containing $3–4\times10^{-5}$ wt% oxygen, protective oxide layers grow on the surface of each candidate alloy and the total thickness of the multiphase layers increases parabolically with increasing exposure time. After 3000 h, they reach a maximum of 50 μm on ferritic steel and 1–2 μm for austenitic steels. In each case the oxide layers prevent the dissolution attack of liquid lead.

For ferritic steels at temperatures below 650 ^{o}C, an increased chromium content increases their corrosion resistance through formation of chrome and/or iron-chrome oxides that protect the steel from attack. This trend is reversed above 750 ^{o}C where the low-chromium steels are more resistant to corrosion. Low-carbon steels suffer moderate penetration in static tests, and their usefulness in a flow system is probably limited to temperatures below 450 ^{o}C [6].

Nickel and nickel containing alloys, such as austenitic steels, are unsatisfactory containment materials for liquid Pb-alloys at temperatures above 500 ^{o}C [7]. This conclusion is attributed to the preferential dissolution of the nickel from the steel into the molten Pb. The Russians [8] have found that steels with relatively low concentrations of nickel (0.8%) and relatively high concentrations of silicon (1.3%) and vanadium (0.4%) seem resistant to corrosion when in contact with molten Pb-alloys at temperatures up to 600 ^{o}C. Gorynin et al. [9] found that the compatibility of steels with Pb–Bi is dominated by two types of corrosion, i.e. corrosion in the Pb–Bi with high-oxygen concentration and so called liquid metal corrosion (LMC) in the Pb–Bi with low oxygen concentration. Between two extreme types of corrosion, there is a possibility of an intermediate condition where steels are slightly oxidized and the formed oxides may suppress the LMC.

One of the primary concerns in using the molten LBE as the coolant, is the degradation of structural materials because the solubility of main elements of structural materials is high in liquid Pb-Bi. Degradation of structural materials occur in various ways: mass transfer, erosion, selective dissolution, compound formation at the surface, oxide formation, liquid penetration at the

grain boundaries, liquid metal embrittlement, etc. Selective dissolution occurs due to the high solubility of certain elements of the steel (Ni, Cr and Fe, mainly) in the liquid LBE . Table 1 shows the solubility of different elements in Pb-Bi [10,11,12].

The concentration of dissolved oxygen or oxygen activity in the liquid metal is a significant parameter on which the corrosion or protection of the structural materials depends [13]. For oxygen concentrations below the equilibrium concentration for the formation of protective layers, the structural steel will suffer dissolution/attack. Upon reaching certain level of concentration of dissolved oxygen corrosion processes is stopped/slowed down due to protective oxide film formed on the steel surface. Oxide films formed on the steel surface prevent it from interaction with liquid metal. On the other hand, if the oxygen concentration is higher than that necessary for formation of oxide layers, the steels as-well-as the liquid metal (Pb & Bi) will undergo oxidation.

Several oxidation/corrosion models of steel in flowing liquid lead or lead-bismuth have been presented. Steel alloying components can dissolve into both aqueous media and liquid– lead alloys [15]. In the past, several methods have been considered to prevent the corrosion problem in LBE. One of the methods is to control the oxygen concentration in the liquid LBE which lead to the formation of a stable oxide layer on the material surface. Another one is to modify the surface of the material or the material compositions [16].

The aim of this work is study the oxidation and corrosion kinetics of different types of steels and inconel alloys in molten lead- bismuth eutectic (LBE) alloy using a static test in the temperature range 450-550 ^{o}C .

Materials and Methods

In this study two type pf stainless steels (304SS and 316 SS) , low alloy steel (Type T_{22}-ASTM) and Inconel 600 alloy (nickel-base superalloy) were used. The nominal composition of these alloys are shown in **Table 2**. Spectrochemical analysis for 316SS, 304S and for Inconel 600 alloy (nickel-base superalloy) was carried out at (Physics Department-College of Science, Baghdad University). The spectrochemical analysis for low alloy steel (Type T_{22}-ASTM) was carried out at the Materials Engineering Department, The University of Technology using metals analyzer type 1650 (ARUN Technology, Germany) , available at the Department of Materials Engineering.

The low alloy steel (Type T_{22}-ASTM) and Inconel 600 alloy `(nickel-base superalloy) alloys samples were cut into squares shape with dimensions (20 mm ×20mm ×4mm) . The stainless steel samples 304SS and 316 SS0 were cut into a disc shape with diameter 10mm and thickness 3.5 mm. Small whole of 2 mm diameter was drilled in each sample for holding. All surfaces, including the edges were wet ground using 120, 220, 320, 600, 800, and 1200 grit silicon carbide papers. These samples were then cleaned with water, degreased with acetone and then ultrasonically cleaned for 30 minutes using ethanol as a medium. After drying, the dimensions of all samples were measured in three

places along the length to a precision ± 0.01 mm using a calibrated micrometer. The weight of each sample was measured using a Mettler microbalance (Switzerland) with an accuracy of ±0.1 mg. The balance was calibrated frequently using standard weights. Prior to weighing, all samples were held overnight in glass desiccator in order to eliminate any effect of humidity on the sample weight determination.

Pb-Bi eutectic alloy (Bi- 56.1 wt % & Pb- 43.9 wt %) was prepared by taking lead and high purity bismuth (99% purity) in the required proportion and melted in an electrical programming furnace. The alloy was homogenized by remelting it three times. The impurities or slag floating on the surface was removed and the alloy was received in the solid form. The samples were kept in an alumina crucible containing LBE which rests inside the alumina tube. In order to evaluate corrosion rate of the steels in the flowing Pb–Bi, the weight losses of specimens caused by the dissolution of the alloying elements into the Pb–Bi or detachment of unstable oxide layer during the exposure into the Pb–Bi were measured. The samples were kept in an alumina crucible. Argon gas flow was maintained over the surface of the LBE melt during the experiment. Four samples of different materials (304, 316, inconel 600 and low alloy steel were exposed in this setup at 450-550 ^{0}C for 100h at 5hrs cycle.

For the measurement of the weight loss, it was necessary to remove adherent Pb–Bi to the specimens, although the oxide layers should not be removed for subsequent metallurgical analysis. It has been found that the immersion of the specimens in a hot glycerin pool is adequate for the removal of adhered Pb–Bi without removing the oxide layers [28]. Thus, in the present study, the adherent Pb–Bi was removed by using a hot glycerin pool for the measurement of weight loss.

Results and Discussion

The specific weight change versus oxidation time for 316SS , 304 SS and inconell alloy in liquid Pb-Bi at 550 ^{o}C are shown in Figure 1-3 respectively. The aim is to establish oxidation correlation for different steel alloys and for Ni-super alloy. Different authors [17, 18, 19, 20] stated that the oxidation correlations gained under gas controlled obeys the same principle mechanism as in liquid Pb –Bi alloys. Under oxidation in liquid metal the vapor pressure is to replaced by solubility. During stainless steels oxidation, the outer-layer (mainly Fe3O4) was due to solid-state diffusion of iron, while the inner layer (mainly Fe–Cr spinel) was due to oxygen reaching the inner surface through micro-pores. The oxidation rate was determined by the diffusion rate through the inner layer where the oxide was compact. The amount of metal diffusing outward consists of two parts: one part forms new oxide at the liquid/oxide interface and the other is removed by liquid. The scale removal by mass-transfer corrosion leads to a high oxidation rate.

Tedmon's Model [19] is based on the Cr oxidation experiments at high temperature with scale vaporization which can be applied to the present oxidation process by replacing the vaporization rate with the mass-transfer-corrosion rate. Tedmon's model is:

$$\frac{d\delta}{dt} = \frac{K_p}{2\delta} - K_r \qquad \text{----------(1)}$$

Where δ is the oxide thickness at time t , Kp is the parabolic-oxide-growth-rate constant , Kr is the scale-removal-rate constant by mass-transfer corrosion rate and is related to the corrosion flux by [17] :

$$K_r = q\frac{\rho_L}{\rho_{ox}(1-f_O)}, \quad \text{----------(2)}$$

Where ρ_L and ρ_{ox} are the density of the liquid and the oxide, respectively, and f_O is the mass fraction of oxygen in the oxide, q corrosion rate (mm/year).

For the zero-oxide-thickness initial condition (no pre-oxidation), the solution of Eq. 1 is [19]

$$t = -\frac{\delta}{K_r} - \frac{K_p}{2K_r^2}\ln\left|1-\frac{2K_r}{K_p}\delta\right|. \quad \text{----------(3)}$$

For non-zero initial condition, $\delta 0 \neq 0$ pre-oxidation), the solution becomes: **[21]**

$$t = -\frac{\delta-\delta_0}{K_r} - \frac{K_p}{2K_r^2}\left[\ln\left|1-\frac{2K_r}{K_p}\delta\right| - \ln\left|1-\frac{2K_r}{K_p}\delta_0\right|\right]. \quad \text{----------(4)}$$

Simplify equation 4 get [17, 21]:

$$\delta = (K_p t)^{1/2} - \frac{2}{3}K_r t, \quad \text{----------(5)}$$

Where δ is the oxide thickness (cm) at time *t (sec)* , *Kp* is the parabolic-oxide-growth-rate constant (cm^2/sec) ,*Kr* is the scale-removal-rate constant by mass-transfer corrosion (cm/sec) . The specific weight change is given by [21]:

$$\Delta W = \rho_{Ox} f_O (K_p t)^{1/2} - \rho_{Ox}\left(1-\frac{1}{3}f_O\right)K_r t \quad \text{----------(6)}$$

Where ΔW is weight change per area (gm/cm^2), *Kp* in (cm^2/sec) and *Kr* in (cm/sec) and f_O is the mass fraction of oxygen in the oxide. ρ_{ox} is the oxide density.

The specific weight change data versus oxidation time in liquid Pb-Bi eutectic at 450, 500, 550 °C for 316SS, 304SS, low alloy steel, and inconell 600 nickel super alloy were fitted first to the parabolic rate equation for oxidation, $\Delta W = K t^n$ and linear rate equation for corrosion $\Delta W = K_1 t$.

Where K is the parabolic rate constant in [gm/($cm^2\sqrt{}$ sec)] and K1 is the linear rate constant in [gm/(cm^2 sec)]. Use the following conversion factors for steel alloys :

K_p (cm^2/sec) x $\{\rho_{ox} f_O\}^2$ = K^2 {$gm^2/(cm^4$ sec)}

Kr (cm/sec) x $\{\rho_{ox} (1- f_O /3\}$ = K_1 {gm/(cm^2 sec)}

Where ρox, is the density of magnetite Fe_2O_3 taken as 5 gm/cm^3, f_O = is the mass fraction of oxygen in the oxide ,

$$f_O = \frac{4M_O}{4M_O + 3M_{Fe}} \quad \text{----------(7)}$$

The curves fitting results for all steel alloys and for inconel alloy at 450, 500, 550 °C, are shown in Table 3-5 . It clear from these tables that n=0.5 for 316SS, 304S and for low alloy. This means that the oxidation process follows a parabolic rate and the values of parabolic rate constants (*Kp*) are tabulated. The results indicate that all steel alloys showed an oxidation/corrosion behavior. The oxidation kinetics is parabolic and the corrosion kinetics is linear. The parabolic rate constant are of the following order $(Kp)_{304SS} > (Kp)_{316SS} > (Kp)_{low\ alloy\ steel}$.

The scale removal rate constant (*Kr*) were also calculated for the three steel alloys 316SS, 304S and for low alloy steel. The specific weight first increases with time and then decreases after it reach a maximum. For inconel alloy, n=1 which means the weight always decreases in time and there is no

oxidation and only corrosion. The scale-removal-rate constants *Kr* are of the following order $(Kr)_{inconel} > (Kr)_{316SS} > (Kr)_{304SS}$.

We attempt to study the oxidation/corrosion behavior of steel alloys in liquid–lead alloy. It is well known that the amount of metal diffusing outward consists of two parts: one part forms new oxide at the liquid/oxide interface and the other is removed by mass-transfer corrosion. The activation energies for oxidation were calculated by plotting Ln Kp versus (1/T) Figure 4. Also the activation energies for scale removal were calculated by plotting Kr versus 1/T Figure 5. The results are tabulated in Table 5.

It was found that the self-diffusion coefficient of iron in Fe_3O_4 can be controlled by either vacancies or interstitials depending on the oxygen level in the liquid–lead alloy. Accordingly, the parabolic-growth-rate constant of Fe_3O_4 can be written as [22]:

$$K_p = \frac{2}{f_{Fe}}\left[D_V (P_{O_2})^{-2/3} - D_I (P_{O_2})^{-2/3}\right]\Big|_{(P_{O_2})_I}^{(P_{O_2})_{II}} \quad \text{---------(8)}$$

where D_V and D_I are diffusion coefficients for vacancy and interstitials respectively , $\mathbf{P_{O2}}$ is the oxygen partial pressure and f_{Fe} **is the** coordinate factor for the self-diffusion mechanism. For Fe_3O_4, the value of f_{Fe} is approximately 0.5 for diffusion mechanism involving vacancy.

Topfer,et al. [22] studied the diffusion coefficient of Fe-and Cr in Fe–Cr spinel for different Cr content and found that the Fe-tracer-diffusion coefficient decreases with increasing Cr content in the spinel. The Cr-tracer-diffusion coefficient is much smaller than that of Fe at the same temperature, therefore during the oxidation process Cr remains at the original locations, while Fe diffuses through the scale to form new oxides. Studies of metal diffusion in the spinel indicate that the diffusion coefficients can be ranked as Mn>Fe>Co>Ni>Cr [23] .

Zhang et al. [17] used equation 8 to calculate the Kp value for 316SS at 550 ^oC , *Kp* [*calculated*] = 3.21×10^{-13} cm^2/s. This value is similar to the values for 316 SS steel calculated by others:

Satio *et al.*[24], *Kp* [*calculated*] =4.75×10^{-14} cm^2/s, and

Smith [25], *Kp* [*calculated*] = 2.64×10^{-13} cm^2/s,

From this work the *Kp* [*calculated*] = 1.8×10^{-13} cm^2/s

It is clear that the calculated Kp from this work is in a good agreement with those calculated from [17, 24, 25]. Unfortunately no other data were available for 304SS and low alloy steel.

Thescale-removal-rate constant (*Kr*) by mass-transfer corrosion is related to the corrosion flux (q) by equation 2 [17]. We attempt to calculate *Kr* and compare it with the experimental value. Based on the analysis of Zhang et al. [26] the corrosion rate *q* is less than 0.01 mm/yr at 550 ^oC for 316SS at oxygen concentration 0.01 ppm. Assuming *q* =0.01 mm/yr, then from equation 9 the Kr [*calculated*] = 1×10^{-14} m/s . From this work, the experimental value for 316SS at 550 ^oC was found to be *Kr experimental* =6.2 $x10^{-14}$ m/sec. The calculated value (*Kr calculated* =1×10^{-14}) by Zhang et al. [26] is smaller than the experimental value (*Kr experimental* = 6.2 $x10^{-14}$), but the difference is deemed acceptable considering there are many uncertainties.

The formation of oxide layers on the steels in the Pb–Bi first could be explained by the reaction of

Fe and oxygen in the Pb–Bi. Then, oxygen in Pb–Bi will diffuse into the steel matrix across the oxide outer layer and then will react chemically with Cr in steel. The oxygen potential in Pb-Bi is higher than that in steel because of the existence of the outer oxide layer as barrier. This oxygen diffusion might produce the stable oxide layer close to the surface of the steel matrix. Once the Cr-rich oxide layer was formed, Fe could not be dissolved easily into the Pb–Bi because of the barrier of the Cr-rich oxide layer [2]

The scale-removal-rate constant (*Kr*) was plotted vs. Ni content is shown in Figure 6. It was found that steel alloys with lower Ni content were only little attacked. A more severe corrosion attack could be found in steels with higher Ni content. With longer exposure time the corrosion rate increases as well. This seems due to the high solubility of Ni in LBE. The solubility of iron, chromium, and nickel in LBE at 500 ^{o}C are 2.3, 11, and 25000 ppm respectively as shown in Table 1 [10,11,12] . For inconel 600 alloy (Ni super alloy) with 74.2 Ni% the corrosion rate is the highest as shown in Figure 6. This is in good agreement with the work of Knebel et al. [27].

The influence of Cr content on the parabolic rate constant Kp of steels tested in LBE at 450 C is shown in Figure 7. The oxidation rate increases with increasing Cr content in the alloy. The 304SS and 316 SS tested under oxidizing Lead–bismuth environment exhibits a thick layer of protective chromium oxide layer at least up to 40 hrs. A high content of chromium at the oxide/steel interface will contribute to the chromium oxide formation. However, after that a deep liquid metal penetration and massive ablation of material by LBE penetration was observed as shown in Figure 8.Our results need more analysis of the cross sections by a scanning electron microscope (SEM) and an energy-dispersive X-ray spectrometer (EDX). The cross section of 316SS oxidized for 100 hrs at 550 ^{o}C in LBEL is showed a spongy appearance. This spongy layer shows deep liquid metal penetration and massive ablation of material at this temperature as shown in Figure 8. This dissolution attack is mainly due to the high nickel content of the steels. As said before, Ni is highly soluble in lead–bismuth.

Conclusions

Under the experimental conditions both steel alloys and inconel 600 alloy exhibited weight loss, and the corrosion was due to the dissolution of alloying elements particularly Ni . The austenitic steels 304SS and 316SS were affected by preferential dissolution of Ni and Cr in the LBE, and the oxidation rate was parabolic and the corrosion rate was linear.

For inconel alloy the corrosion rate was linear and this alloy suffer sever corrosion in LBE.

References

[1]. K. Chandra and Vivekanand Kain, "Compatibility of Different Stainless Steels in Molten Pb-Bi Eutectic at High Temperatures", International Conference on Corrosion CORCON, Chennai, India, 2005.

[2]. Masatoshi Kondo, Minoru Takahashi, Naoki Sawada and Koji Hata, "Corrosion of Steels in Lead–Bismuth Flow" , Journal of Nuclear Science and Technology , Vol. 43, No. 2, p. 107–116, (2006)

[3]. Eric P. Loewen and Akira Thomas Tokuhiro, "Review, Status

of Research and Development of the Lead-Alloy-Cooled Fast Reactor" J. of Nuclear Science and Technology, Vol. 40, No. 8, p. 614–627, August 2003

[4] . N. Li, "Active Control of Oxygen in Molten LBE Systems to Prevent steel corrosion and coolant contamination," J. Nucl. Mater. 300, pp 73–81, (2002).

[5]. H.Glasbrenner, J.Konys,G.Mueller, A.Rusanov, "Corrosion Investigations of Steels in Flowing Lead," J. Nucl. Mater.,Vol **296**, pp 237–242 (2001).

[6]. J. L. Everhart, E. L. Van Nuis," Liquid Metal Heat Transfer Fluid Unstressed Static Corrosion Tests", NP-1497, U.S. Atomic Energy Commission, (1950).

[7]. I. Kinoshita, "Liquid metal cooled small reactors (MDP and 4S) In CRIEPI," International Seminar on Status and Prospects for Small and Medium Sized Reactors, Cairo, Egypt, May 27–31, 2001.

[8]. E. Adamov, V. Orlov, "Nuclear power at the next stage: Cost-effective breeding, natural safety, radwastes, nonproliferation," Nucl. Eng. Des., **173**, pp. 33–41, (1997).

[9]. I. V. Gorynin, G. P. Karzov, V. G. Markov, V. S. Lavrukhin,V. A. Yakovlev, ''Structural materials for power plants with heavy liquid metals as coolants,'' Proc. HLMC1998, Obninsk, Russia, Oct. 5–9, p. 120, (1998).

[10]. Ph. Deloffre, A. Terlain, F. Barbier, "Corrosion and Deposition of Ferrous Alloys in Molten Lead-bismuth", Journal of Nuclear materials, Vol. 301, p. 35, 2002

[11]. John J. Park, Darryl P. Butt, Carl A. Beard, Design and performance of Reactor and Sub critical Blanket systems with Lead and Lead Bismuth as Coolant and or Target Materials .Nucl. Eng. Design, Vol. 196, p. 315, 2000.

[12]. C. Fazio, I. Ricapito, G. Scaddozzo, G. Benamati, "Corrosion Behaviour of Steels and Refractory Metals and Tensile Features of Steels Exposed to Flowing Pb-Bi in the LECOR Loop", J. Nuclear . Materials . Vol. 318, p.325, 2003.

[13]. IAEA-TECDOC-1289, Comparative Assessment of Thermophysical and Thermohydraulic haracteristics of Lead, Lead-bismuth, and Sodium Coolants for Fast Reactors, International Atomic Energy Agency Report , Vienna (Austria), June 2002.

[14]. J. U. Knebel, X. Cheng, C. H. Lefhalm, G. Müller, G. Schumacher, **J.**Konys and H. Glasbrenner **,** "Gas-phase oxygen control processes for lead/bismuth loops and accelerator driven systems" (ADS). Nucl. Eng. Design, Vol. 202, p.279, 2000.

[15]. B. Stellwag, Effect of Surface Roughness of Steels on Oxide Layer Formation in a Liquid Lead-Bismuth Flow, Corrosion Science**, Vol. 40**, p.337, 1998

[16]. Gorynin, V., G.P. Karzov, V.G. Markov V.A. Yakovlev ,"Structural Materials for Atomic Reactors with Liquid Metal Heat-transfer Agents in the Form of Lead or Lead-bismuth Alloy", Metal Science and Heat Treatment, Vol. 41, No 9-10, pp. 384-388, 1999.

[]17]. J.Zhang and N.Li ,Oxidation Mechanism of steels in Liquid –Lead Alloys ,Oxid of Metals , Vol63, Nos.5/6, p.353, June 2005

[18]. G.Muller, G. Schumacher, F. Zimmermann (2000), "Investigation on Oxygen Controlled Liquid Lead Corrosion of Surface Treated Steels", Journal of Nuclear Materials, Vol. 278, pp. 85-95

[19]. C.S. Tedmon Jr, "Oxide Protection of Materials in Melts of

Lead and Bismuth", J. of Electrochemical Soc., Vol.113, p.766, 1966.
[20] .J. Robertson, Corrosion Science, Vol.32, p. 443 , 1991.
[21]. H. Taimatsu, Design Study of Pb-Bi-Cooled and NaK-Cooled Small Reactors: PBWFR and DSFR , J. Electrochemical Soc., Vol.146, p. 3686 , 1999.
[22]. J. Topfer, S. Aggarwal, and R. Dieckmann, , "Oxide Layer Stability in Lead-bismuth at High Temperature" Solid State Ionics, **Vol.81**, p.251, 1995.
[23]. J. Robertson, , "Control of Oxygen Concentration in Liquid Lead and Lead-bismuth, Corrosion Science**, Vol. 29**, p.1275 ,1989.
[24]. M. Saito, H. Furuya, and M. Sugisaki, "Investigation on Oxygen Controlled Liquid Lead Corrosion of Surface Treated Steels" J. Nuclear Materials **Vol.135**, p.11, 1985.
[25]. A. F. Smith, "Short-term Static Corrosion Tests in Lead-bismuth", Corrosion Science**, Vol. 22**, p.857, 1982.
[26]. J. Zhang, N. Li, Parametric Study of a corrosion model applied to lead-bismuth flow systems, *Journal of Nuclear materials*, Vol. 321, 184 (2003).
[27]. J.U. Knebel, X. Cheng, G. Müller, G. Schumacher, J. Konys, H. Glasbrenner **,** "Thermalhydrualic and Corrosion challenges for the Target Module of an Accelerator-Driven System ",Third International Topical Meeting on Nuclear Application of Accelerator Technology AccApp'99, Long Beach CA, November 14-18, pp.367-376, 1999.

Table 1 Solubility of different elements in Pb-Bi [10,11,12].

Elements	Molten Pb		Molten Pb-Bi		Molten Bi	
	ppm	Temp.,	ppm	Temp.,	ppm	Temp.,
Fe	2.6	600	10	600	50	600
	0.8	500	2.3	500	15	500
Cr	730	600	11	500	150	600
Ni	5370	600	25000	500	66000	600

Table 2 Chemical compositions (in wt.%) of steels and Inconel 600 used in present work.

Materials	Cr	Ni	Mo	Mn	Si	C	Al	Fe
316SS	16.8	10.4	2.04	0.92	0.66	0.06	-	Rem
304SS	18.5	9.2	-	1.36	0.85		-	Rem
Low alloy steel Type T_{22}-ASTM	1.96	---	0.91	0.35	0.46	0.06	-	Rem
Inconel 600	15.9	Rem	0.5	0.1	0.2	0.1	0.399	8.4

Table 3. Kp and Kr values for different steel alloys and Inconnel 600 oxidized in LBE at 450 °C

Materials	K gm/(cm^2√ sec)	n	K_P (cm2/sec)	K1 gm/(cm^2 sec)	K_r (cm/sec)
316SS	$2x10^{-7}$	0.55	$2x10^{-14}$	$3.45x10^{-10}$	$7.6x10^{-11}$
304SS	$4x10^{-7}$	0.45	$8x10^{-14}$	$1.54x10^{-10}$	$3.4x10^{-11}$
Low alloy steel	$1x10^{-7}$	0.53	$5x10^{-15}$	$3.3x10^{-10}$	7.3E-11
Inconel 600	------	------	----	$9x10^{-6}$	$1.29x10^{-10}$

Table 4. Kp and Kr values for different steel alloys and Inconnel 600 oxidized in LBE at 500 °C.

Materials	K gm/(cm^2√ sec)	n	K_P (cm2/sec)	K1 gm/(cm^2 sec)	K_r (cm/sec)
316SS	$4x10^{-7}$	0.59	$8x10^{-14}$	$7.7x10^{-10}$	$1.7 x10^{-10}$
304SS	$7x10^{-7}$	0.5	$2.45 x10^{-13}$	$3.82x10^{-10}$	$8.4x10^{-11}$
Low alloy steel	$3x10^{-7}$	0.47	$4.5x10^{-14}$	$1x10^{-9}$	$2.2x10^{-10}$
Inconel 600	------	------	----	$5x10^{-9}$	$7.14x10^{-10}$

Table 5. Kp and Kr values for different steel alloys and Inconnel 600 oxidized in LBE at 550 °C

Materials	K gm/(cm$^2\sqrt{}$ sec)	n	K_P (cm2/sec)	K1 gm/(cm^2 sec)	K_r (cm/sec)
316SS	$6x10^{-7}$	0.55	$1.8x10^{-13}$	$2.8x10^{-9}$	$6.2\ x10^{-10}$
304SS	$1.02x10^{-6}$	0.5	$5.2x10^{-13}$	$1.13x10^{-9}$	$2.5x10^{-10}$
Low alloy steel	$2.53x10^{-7}$	0.47	$3.2x10^{-14}$	$2x10^{-9}$	$4.4x10^{-10}$
Inconel 600	------	------	----	$1x10^{-8}$	$1.43x10^{-9}$

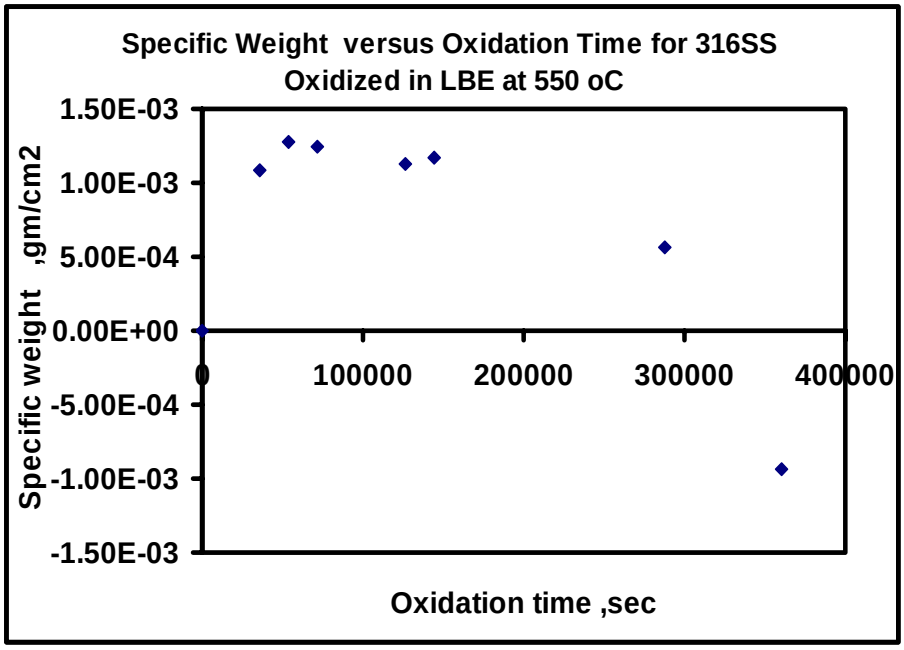

Figure (1). Specific weight versus oxidation time for 316SS at 550 °C in LBE

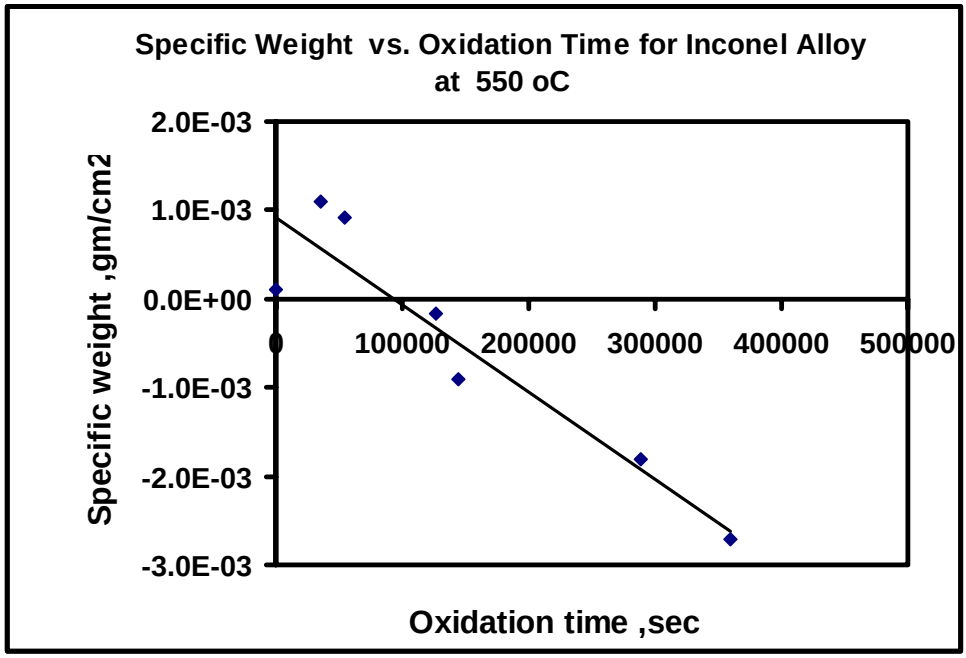

Figure (2). Specific weight change versus oxidation time for inconel 600 at 550 ^{o}C in LBE

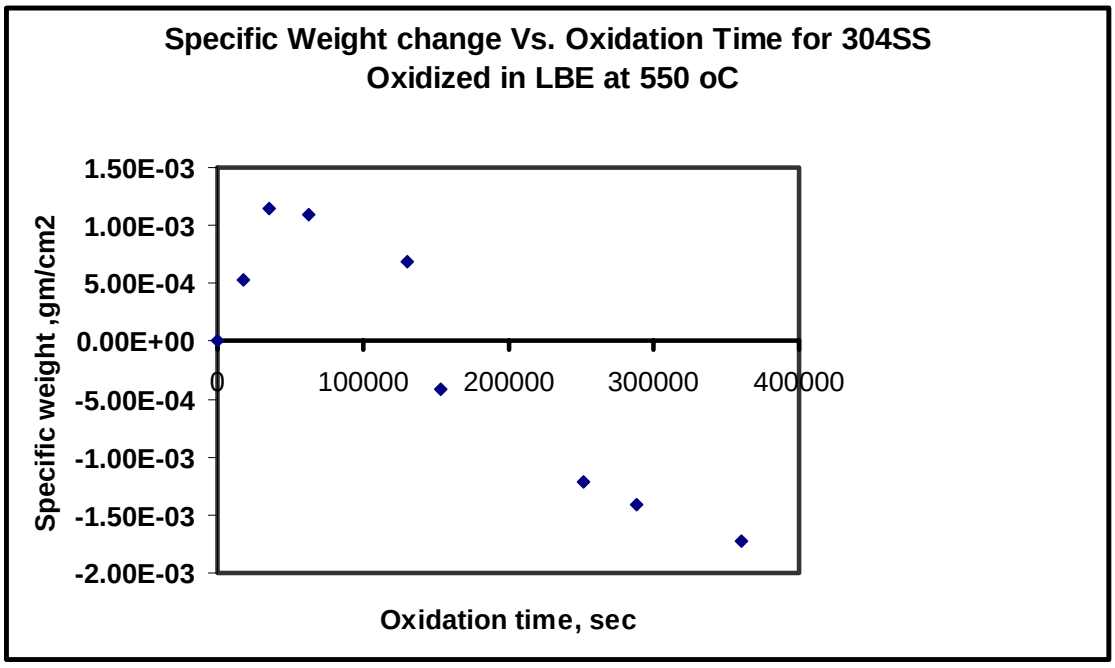

Figure (3). Specific weight change versus oxidation time for 304 SS at 550 ^{o}C in LBE

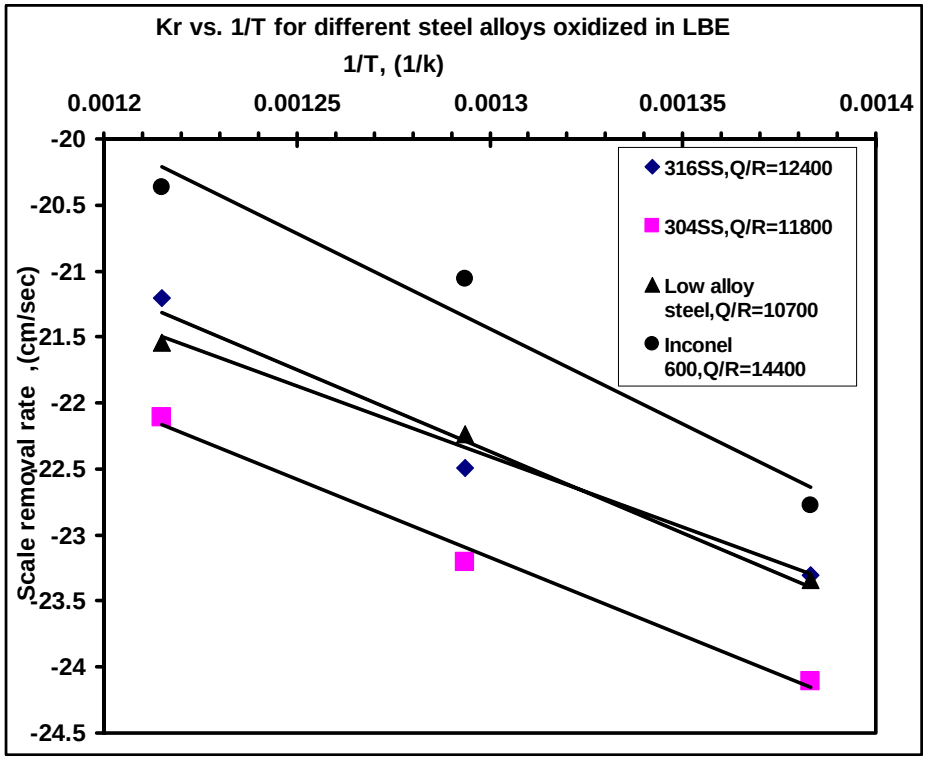

Figure(4). The scale-removal-rate constant (*Kr*) vs. (1/T) for different steels and inconel alloy oxidized in LBE at 450-550 ^{o}C for 100 hrs.

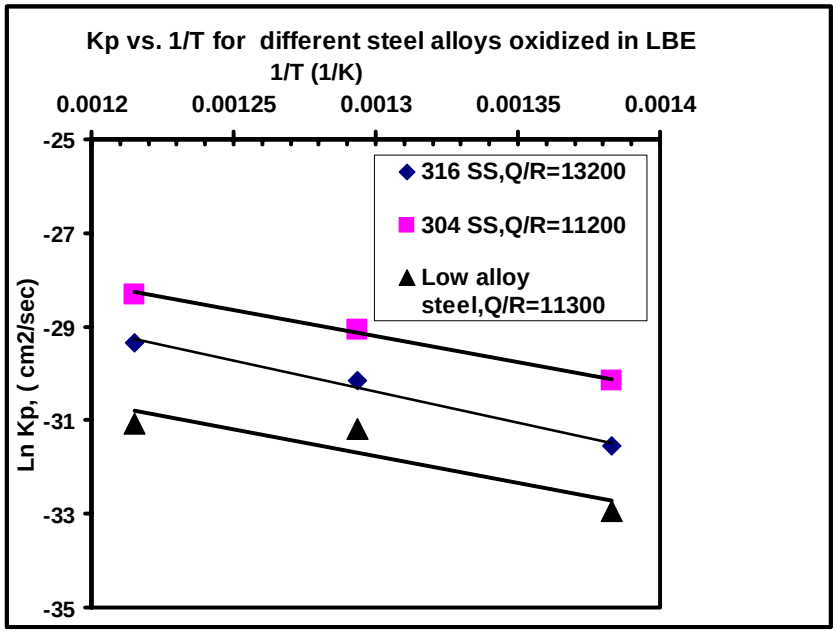

Figure(5). The parabolic rate constant (*Kp*) vs. (1/T) for different steels oxidized in LBE at 450-550 ^{o}C for 100 hrs..

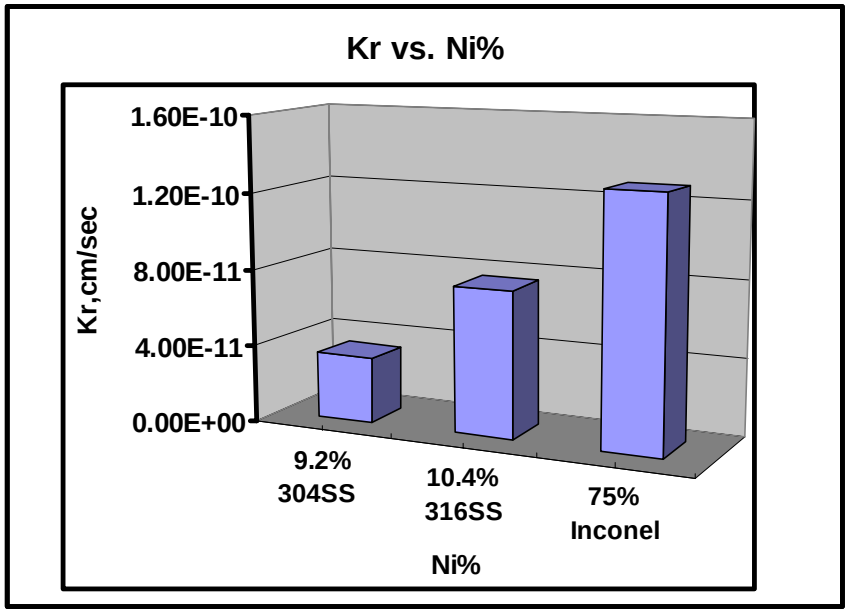

Figure(6) Scale removal rate constant vs. Ni% for different alloys oxidized at 450 ^{o}C in LBE.

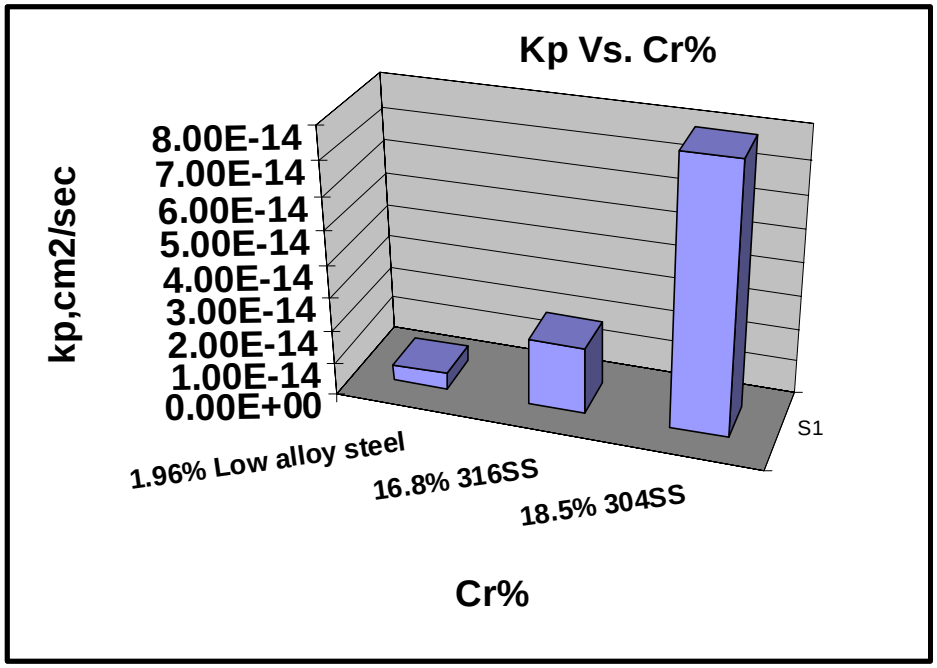

Figure (7) Parabolic rate constant vs. Cr% for different alloys oxidized at 450 ^{o}C in LBE.

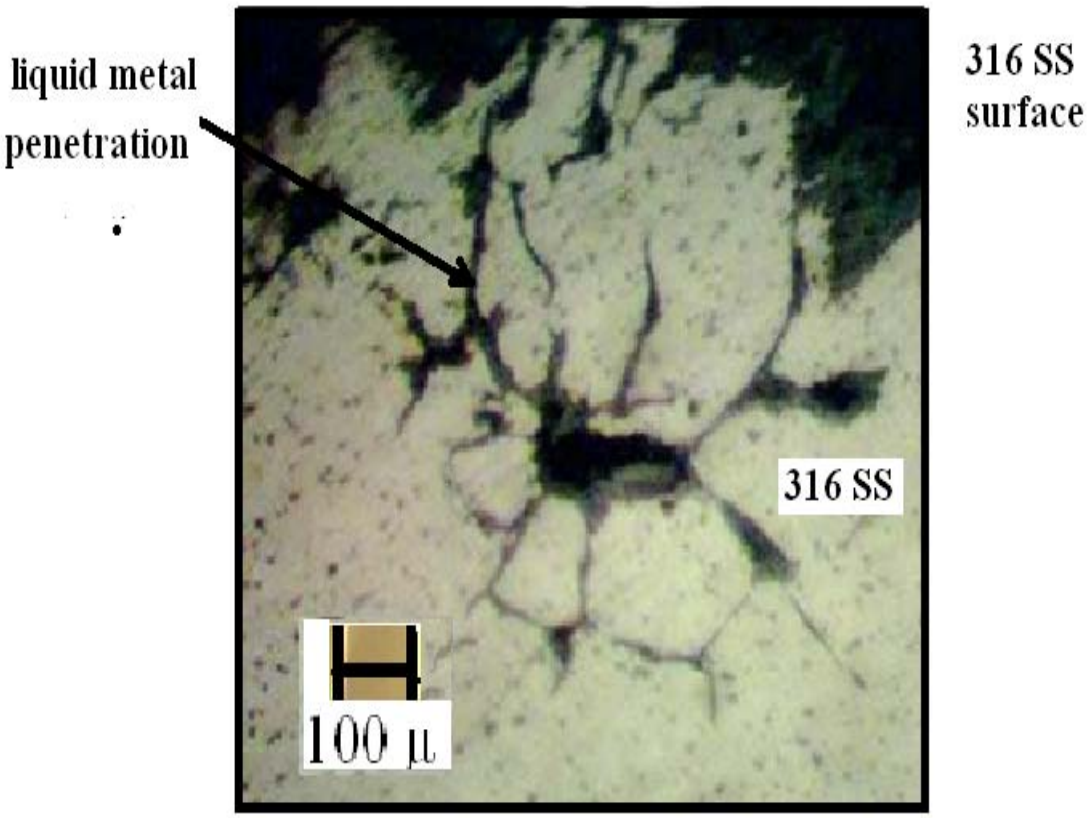

Figure (8) . Lead-Bismuth penetration in 316SS after 100 hrs oxidation at 550 ^{o}C.